Research Article Adv. Mat. Lett. 2012, **3**(3), 220-225 ADVANCED MATERIALS Letters

www.vbripress.com, www.amlett.com, DOI: 10.5185/amlett.2012.1309 Published online by the VBRI press in 2012

Low temperature synthesis and magneto resistance study of nano $La_{1-x}Sr_xMnO_3$ (x = 0.3, 0.33, and 0.4) perovskites

Maneesha Gupta[1, 2,*], Poonam Yadav[3], Wasi Khan[1], Ameer Azam[1,4], Alim H. Naqvi[1], R.K. Kotnala[3]

[1]*Center of Excellence in Materials Science (Nanomaterials), Department of Applied Physics, Z.H.C.E.T, A.M.U., Aligarh 202 002, India*
[2]*Space Applications Center, ISRO, Ahmedabad 380 015, India*
[3]*National Physical Laboratory, Pusa Road, New Delhi 110 012, India*
[4]*Centre of Nanotechnology, King Abdulaziz University, Jeddah, Saudi Arabia*

[*]Corresponding author. Tel: (+91) 9375031959; Fax: (+91) 79-26914796; E-mail: maneesha.nano@gmail.com

Received: 09 January 2012, Revised: 12 February and Accepted: 13 April 2012

ABSTRACT

We have synthesized $La_{1-x}Sr_xMnO_3$ (with x=0.3, 0.33 & 0.4) perovskite nanoparticles using mild sol-gel technique at low temperature and thereby studied the effect of nanosize on magnetoresistance. These samples were characterized using TGA/DSC, XRD, TEM, FTIR and temperature dependent magnetoresistance (MR) measurements. Powder X-ray diffraction (XRD) result confirms the formation of pure crystalline phase with rhombohedral symmetry in R-3C space group. Crystallite size increases with increase in Sr concentration. TEM analysis further supports the nanosized particles in the samples which lie in the range of 20-30 nm. Fourier transform infrared (FTIR) spectroscopy shows a broad peak at 615 cm^{-1} for all the samples gives an evidence for the formation of metal oxygen bond organized in to MnO_6 octahedral. The steep change in magnetoresistance (MR) at low field at low temperature is observed which is attributed to the alignment of the spins, while in the high field MR is due to the grain boundaries effect at low temperature. In the series studied, 33% Sr doped sample shows higher MR both at low temperature (-17.15) and room temperature (-3.07) than their counter parts. Copyright © 2012 VBRI Press.

Keywords: Manganite; sol-gel process; magnetoresistance; citric acid.

Maneesha Gupta is presently working as Scientist at Space Applications Center, ISRO, Ahmedabad, India. Together with she is pursuing her PhD degree in perovskites nanomaterials from Department of Applied Physics, Aligarh Muslim University (AMU), Aligarh, India (Registered january 2008). She obtained her Masters degree in Physics (2007) from Department of Physics, AMU, Aligarh. In her four years of research she has synthesized and characterized various doped perovskites materials in bulk as well as in nano domain. Her interest is in developing and designing Nanomaterials for space applications..

Alim H. Naqvi is Professor of Applied Physics. He is also Coordinator of Centre of Excellence in Materials Science (Nanomaterials) and M. Tech. Nontechnology Programme in Aligarh Muslim University, Aligarh, India. His research interest lies in the development of nanocomposite materials and their applications.

Ameer Azam obtained his Master degree in Physics (1983) from Meerut University, Meerut and M.Phil. (1987) & Ph.D. (2002) received in Applied Physics from Aligarh Muslim University, Aligarh, India. He joined the Department of Applied Physics as Assistant Professor in 1996 and was promoted as Associate Professor in 2006. He has published more than 60 papers in National/International refereed Journals. Currently, he is on sabbatical leave and working as Associate Professor in Centre of Nanotechnology, King Abdulaziz University, Jeddah, Saudi Arabia. At present, his work mainly involves synthesis, characterisation and applications of nanomaterials.

Introduction

The rare earth manganite perovskite with general formula $La_{1-x}A_xMnO_3$ (A = Ba, Sr, Pb and Ca) are of high technological and scientific interest due to their spectacular physical properties and versatile field of applications such as magnetic-field sensor [**1, 2**], hard disk read heads [**3**], fuel cells [**4, 5**], infra-red devices [**6**], spintronics materials, memory devices (electroceramics), micro-wave active components, magnetocaloric refrigeration [**7**], magnetically guided drug delivery and hyperthermia *etc*. because of remarkable phenomenon occurring in these systems such as John teller distortion, Double exchange, charge ordering (CO), orbit ordering, spin ordering and magnetic ordering. Double exchange effect is an exchange of electrons from neighboring Mn^{3+} to Mn^{4+} ions through oxygen when their core spin are parallel and hopping is not favored when they are anti-parallel. However, it has been claimed that an additional mechanism, Jahn-Teller distortion (JT) could be responsible for the transport properties. In general, CMR effects of polycrystalline ceramic bulk exhibit two classes of magnetoresistance (MR), the intrinsic and extrinsic MR. The former is referred to intra-grain effect where its MR shows a maximum near paramagnetic-ferromagnetic transition temperature (T_c) and maximum electrical resistivity at metal-insulator transition temperature (T_p). The latter is due to the intergrain effect where higher MR could be observed over a wider temperature range below Tc and is characteristic of a Low-Field MR (LFMR), which is believed to be due to Spin-Polarized Tunneling (SPT) or Spin-Dependent Scattering (SDS) of conduction electrons across grain boundary [**8-10**]. Recently, the effect of grain boundaries in the polycrystalline manganites has been studied intensively, where the grain's shape or microstructure will be changed with different preparation process or dopant. It is found that substitution of divalent atoms with variance atomic radius and synthesis process will influence the magnetic properties and electrical properties of the system [**11, 12**].

Furthermore, the magnetic properties of nanoparticles strongly depend on the size and shape of particles, particle size distribution, finite-size effect and dipolar or exchange interaction between the particles[**13-16**] thus it is important to know the effects of interaction between nanoparticles on physical properties of these systems [**15, 17**]. If the particle size is smaller than the size of single domain, each particle has a large magnetic moment (so-called super spin) [**13, 16, 17**] which is good for hyperthermia application [**18**], where magnetic nanoparticles of fairly uniform size, having a Curie temperature above room temperature nearly 45^0C, are needed. Doped manganites LSMO can be an interesting material in this context due to its high T_c value (about 380 K) and a large magnetic moment at room temperature [**19-22**] with good CMR properties. Further, it is widely accepted that the dopant concentration x and the band width (or the tolerance factor) are dominant two parameters which enable us to systematically tune the magnetic and transport properties including the colossal magnetoresistance (CMR) and metal-insulator transition accompanied by the charge and orbital order (CO). The fact that these enchanting properties are significantly influenced by the A-site randomness motivated us to develop the A-site ordered manganites without the A-site randomness. This nanosized manganite can be synthesized by various methods like homogeneous Co precipitation, Solo thermal decomposition, hydrothermal [**23-25**], microemulsion technique, anodized alumina oxide (AAO) *etc.*

In this study, an effort has been made to synthesize Sr doped $LaMnO_3$ system in nano regime i.e. $La_{1-x}Sr_xMnO_3$ (x = 0.3, 0.33 & 0.4) nanoparticles (NPs) using mild sol gel approach at a low temperature and further to investigate the influence of Sr (as a divalent atoms substituted at A site) on the magnetoresistance. In our approach out of various synthesis methods mentioned earlier this is a preferable alternative due to very short reaction time, simple synthetic apparatus and simple operating procedure. This method also allows synthesis of LSMO NPs in large scale up to several tenth grams. Strontium as a dopant controls the number of carriers, actually holes, at the Fermi level. At the optimal doping that we considered in this work LSMO is a robust ferromagnet with Curie temperature well above room temperature.

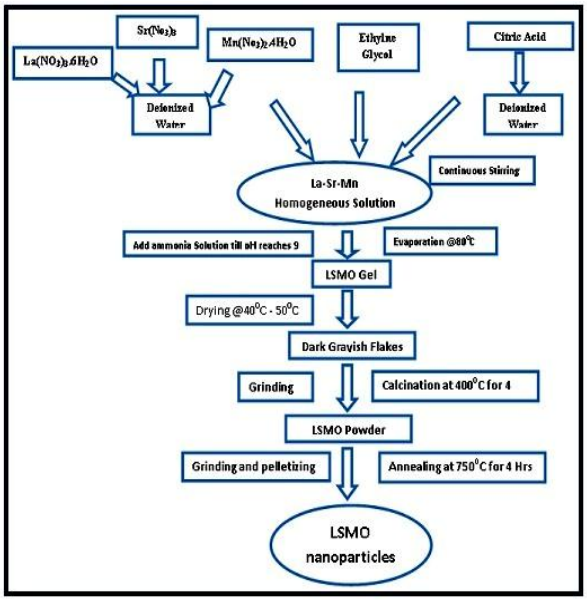

Fig. 1. Schematic illustration of the preparation of Sr doped $LaMnO_3$ nanoparticles by sol-gel method.

Experimental

The LSMO nanoparticles $La_{1-x}Sr_xMnO_3$ (with x = 0.3, 0.33 & 0.4) were synthesized by sol-gel procedure from their nitrate precursors. GR grade starting compounds $La(NO_3)_3.6H_2O$ (G.S Chemicals, 99.9%), $Sr(NO_3)_3$ (Alfa Aesar, 99%), $Mn(NO_3)_2.4H_2O$ (Across, 99.9%), were dissolved in deionized water in a separate beaker than it is mixed with the solution of citric acid ($C_6H_8O_7$, chelating legend) (Fisher, 99.9%) and ethylene glycol, at constant stirring, in the ratio of (1-x[La^{3+}]+x[Sr^{2+}]+1[Mn^{2+}])/1.5[citric acid]/2.25[ethylene glycol] to get a transparent stable solution as shown in **Fig. 1.**

Ammonia solution was added drop wise to the solution till the pH reached 9. The solution was then heated on a hot plate under constant stirring at 80^0C to eliminate excess water and the resulting solution was converted into viscous glassy gel. The gel was then dried at 40-50^0C to get dark

grayish flakes. The flakes were ground to get as-prepared powder of Sr doped $LaMnO_3$. The powder was calcined at 400^0C for 4 hours in box furnace. The calcinated samples were again ground and were converted into pellets at 8-9 tons/cm^2 pressure. These pellets were further annealed at 750 ^{0}C for 4 hours to get the desired manganite nanoparticles. The thermogravimetric analysis (TGA) and differential thermal analysis (DTA) were carried out with Mettler Toledo at the heating rate of 10^0C/ minute in air. The structural characterization (phase formation, lattice parameters and crystallite size) was performed by X-ray diffraction (XRD) using Rigaku (Miniflex-II) diffractometer with CuK_α (λ=1.5418 Å) radiation. To know the chemistry of formation of Sr doped $LaMnO_3$ nanoparticles, Fourier transform infrared (FTIR) spectroscopy was undertaken over the frequency range 400-4400cm^{-1} (the powder sample were diluted by KBr and pressed in to a disk of thickness 0.1mm). The morphology and size of the grains were directly investigated by high resolution transmission electron microscopy (HR-TEM) using JEM 200CX (Jeol). The magnetoresistance (MR) of the samples from 77K to 300K was measured by the standard four-probe method where a constant current of 1 mA was passed through the sample from a dc current source (Keithley, model 8330) and with a field variation from 0 to 8000 Oerested (using Bruker electromagnet) corresponding voltage drop across the sample was recorded with a Keithley (model 181) nanovoltmeter.

Results and discussion

Thermogravimetric and differential thermal analysis (TGA/DSC)

Thermogravimetric Analysis (TGA) and Differential Thermal Analysis (DTA) of 33% Sr doped sample are shown in **Fig. 2.** Exothermic one-step decomposition of the nitrate/citrate complexes takes place in the temperature range 300 °C < T < 400 °C. With the increase in temperature there are three weight loss regions observed in the TGA curve. According to the quantity calculation of the weight loss in each region, the whole thermal decomposition process can be distinguished below. The weight loss region in the temperature range ~35-105^{0}C is 6% which is due to loss of coordinate and solvent water molecules. The weight loss between 150 to 320^{0}C is ~5 % which is due to decomposition of nitrates/citrates around 300^{0}C and decomposition of CH_x organic components. The third stage of TGA is a fast weight loss stage with 30% loss between 420-650^{0}C which is due to the decomposition of burning of residual organic compounds of the precursor. Above 650^{0}C there is no mass change in TGA curve suggesting the crystallization and formation of perovskite phase which was also confirmed by XRD and TEM. According to above data we decided to sinter the samples at 750^{0}C.

Structural characterization

Fig. 3 shows XRD patterns of all the Sr doped $LaMnO_3$ samples calcinated at 400^{0}C and sintered at 750^{0}C for 4 hours by sol-gel method in the 2θ range 20-80^0. It is evident from the patterns that all the samples are formed in single phase without showing any secondary or impurity phases. However, the XRD peaks of these powders were very broad with large full width at half maxima (FWHM) indicating formation of fine LSMO nano powders. The patterns were similar to that of perovskite structure i.e. orthorhombic ABO_3 with space group R3c. The diffraction peaks at angle 2θ ~32.07 represents the (110) plane of perovskite phase.

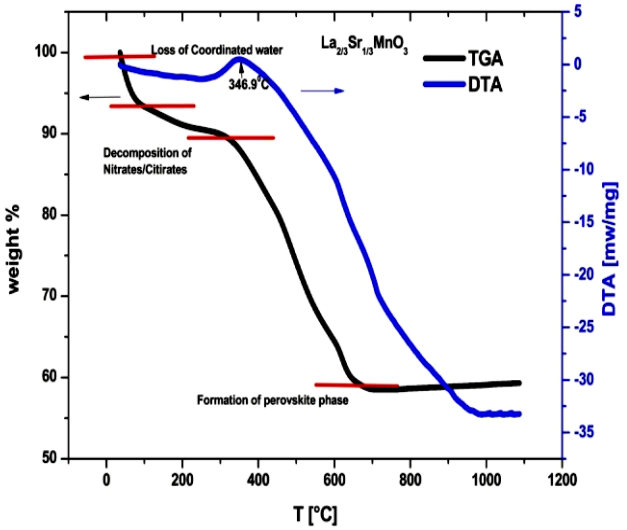

Fig. 2. TGA and DTA curves of $La_{2/3}Sr_{1/3}MnO_3$ precursor by sol gel technique.

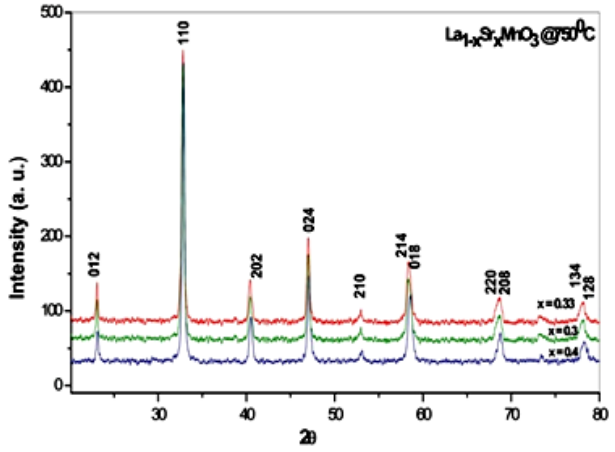

Fig. 3. XRD patterns of Sr doped $LaMnO_3$ for x= 0.3, 0. 33 and 0.4 samples sintered at 750 °C.

Table 1. MR (8kOe) and LFMR (1.6kOe) variation with particle size and doping concentration at 77K and 300 K.

Composition x	Crystallite Size (t)	MR% at 77K and at 8000Oe	MR % at 300K and at 8000Oe	LFMR at 77K and at 1.6 KOe	LFMR at 300K and at 1.6KOe
0.3	24.07	-16.064	-3.02728	-10.9641	-1.10279
0.33	24.28	-17.157	-3.07284	-13.7617	-1.07305
0.4	29.86	-11.9468	-1.57134	-6.40021	-0.36973

The average crystallite size *(κ)* was determined using the Debye Scherrer's equation $\kappa = 0.9\lambda/\beta\cos\theta$, where λ is the incident X-ray wavelength (λ_{Cu}=1.5443 Å), β is full width at half maximum (FWHM) of the peak corresponding to maximum intensity and θ represents the diffraction angle of

the most intense peak in degrees. The crystallite sizes (κ) of the LSMO samples for different doping of Sr are given in **Table 1** suggesting the systematic broadening of peak or in turn the particle size with doping concentration. The average crystallite size (κ) of the LSMO samples lies in between 24 to 30 nm.

However, the procedure of finding average crystallite size using Scherrer's formula is an indirect way to estimate the size approximately. Structural characterization using TEM is rather a direct and appropriate way to find the grain size exactly. **Fig. 4** shows TEM bright field image of LSMO nanocrystalline samples comprising narrowly distributed particles. The average particle sizes estimated from the micrograph considering the minimum and maximum diameter of large number of particles was found to be in the range of 20 to 30 nm for x =0.3 and x=0.33 respectively, which is the best as reported so far at this temperature, to the best of our knowledge. Thus, TEM shows almost the same particle size for low doping concentration i.e. $x \leq 0.33$ as calculated from XRD. The size for x=0.4 size lies between 40 to 50 nm which is due to congregation/agglomeration of the particles. Agglomeration could be explained on the fact that precursor powder contains large amount of organic compounds, which may increase the temperature in the system during thermal treatment.

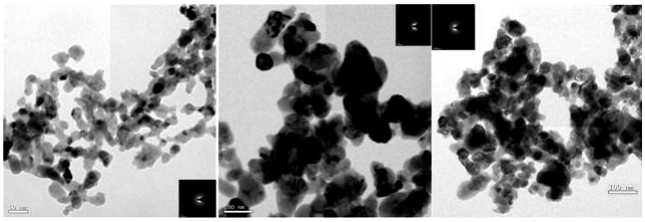

Fig. 4. TEM bright field images with corresponding selected area electron diffraction (SAED) patterns (inset) of $La_{1-x}Sr_xMnO_3$ for (a) x=0.3 (b) x=0.33 (c) x=0.4 samples.

The inset of **Fig. 4** shows corresponding selected-area electron diffraction (SAED) patterns of the same sample. The SAED pattern reveals spotty ring patterns, indicating its crystalline structure and is in good agreement with XRD results.

Fourier transform infra-red spectroscopy (FTIR)

The FTIR transmission spectra of the Sr doped $LaMnO_3$ prepared by using citric acid and ethylene glycol, dried at 80 ^{0}C (As prepared and sintered at 750 ^{0}C) recorded with KBr pellet are shown in **Fig. 5** (a) & (b) represents the chemistry for the formation of LSMO perovskite materials by sol-gel method.

As seen from **Fig. 5** (a) & (b) a broad adsorption band around 3448 cm^{-1} appeared in the IR spectra of all citric acid-ethylene glycol-salt resins, which are characteristic of absorbed water or hydroxyl group in alcohol (O-H stretching). The absorption peak at 1637 cm^{-1} and 2344 cm^{-1} are due to the deformation mode of absorbed molecular water of the carrier KBr $(H_2O)_n$ and CO_2 respectively [**26**]. Figures also show a clean FTIR spectrum with an absorption peak at 615 cm^{-1} corresponding to the stretching mode, which involves the internal motion of a change in

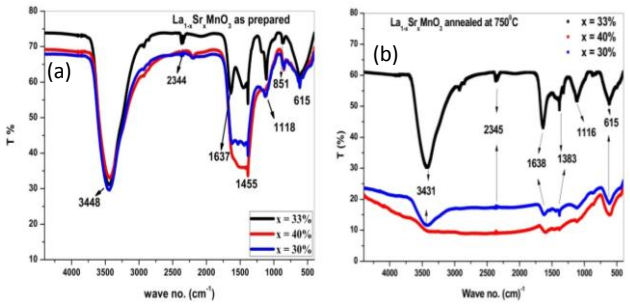

Fig. 5. FTIR spectra of Sr doped $LaMnO_3$ Samples for x= 30%, 33%, 40% (a) as prepared (b) annealed at 750 $^{\circ}$C.

Mn-O-Mn bond length [**27**] and this metal oxygen bonds are subsequently organized into a MnO_6 octahedral structure, as evidenced by the appearance of a well-defined spectral band at about 615 cm^{-1}. This represents the formation of crystalline powder containing the LSMO perovskite structure material, which is in agreement with the result of XRD [**28**]. In as prepared strong absorption peaks at 851 cm^{-1} and 1455 cm^{-1} are due to $SrCO_3$ which diminishes with sintering. A strong band near 1118 cm^{-1} reveals the formation of CH_3-CH_3-, CH_3-NH_2-, CH_3-O- bands when the polymerization takes place with metal nitrate, citric acid and ethylene glycol. This band 1118 cm^{-1} also attributed to the C-C-O structure from ethylene glycol in the polymerization process. The resin was characterized to have both monodentate and bidentate ligand of carbonyl group, which may be due to the fact that the resins contain the chelating of carbonyl group with metal ions. Additionally, in annealed LSMO samples with the absorption bands in the vicinity of 1383 cm^{-1} reveals the existence of carbonate. From the characteristic stretching vibration peaks of carbonyl group the presence of a lot carbonate can be noticed. From the FTIR analysis, it can be suggested that the ethylene (C-C-O) readily undergoes oxidation than citric acid.

Magnetoresistance (MR) measurements

MR study for the present series of LSMO samples has been carried at room temperature (300K) as well as at low temperature (77K). Magnetic measurements as shown in **Fig. 6** exhibited the magnetic field dependent behavior of MR having crystallite size, κ =24.07, 24.28 and 29.86 nm by varying the applied magnetic field from 8 to -8 kOe. The MR measured values corresponding to doping and crystallite size is shown in table 1. At temperature of 77K and 300K the curves exhibited distinct LFMR, characterized by a sharp drop of MR at low fields (H<1.5 kOe), followed by a slower varying MR at a comparatively high-field regime (H>1.5 kOe) where MR is almost linear with H. This LFMR is governed by spin polarized tunneling (SPT) transport of conduction electrons across grain boundaries [**29**]. **Fig. 7** shows variation of MR with doping Concentration at Applied field of 8kOe. It is interesting, that with doping concentration within 30 to 40 % both LFMR and MR (8kOe) are good in case of 33 % Sr doped $LaMnO_3$ sample though 30 % doped sample has smaller

crystallite size than 33% doped sample. This shift in magnetoresistance at all fields can be due to the fact that with decrease in κ MR increases until the nanoparticles remain in magnetically multi domain regime, but as soon as it falls in the single domain regime, MR immediately starts diminishing [**30, 31**].

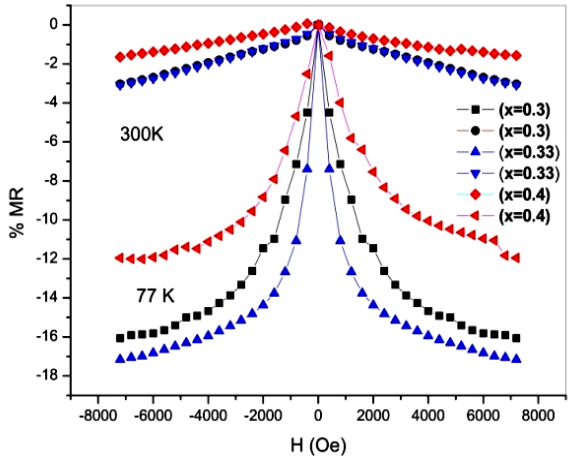

Fig. 6. Magnetoresistance of $La_{1-x}Sr_xMnO_3$ with x = 0.3, 0.33 and 0.4 samples in 77 and 300K.

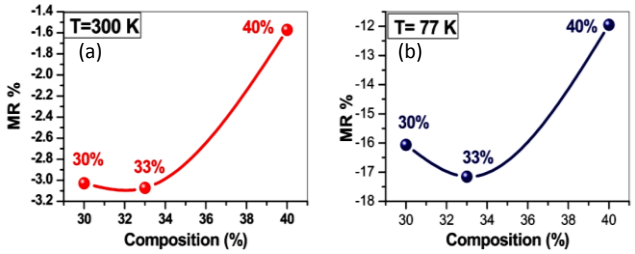

Fig. 7. MR variation with Sr doping concentration at A site of $LaMnO_3$ at applied field of 8KOe (a) 300K and (b) 77K.

Conclusion

In order to maintain the phase and magnetic properties of the perovskite a reproducible low temperature synthesis method was performed to synthesize $La_{1-x}Sr_xMnO_3$ with $0.3 \leq x \leq 0.4$ nanoparticles in the range 20 to 50 nm. Thus, particle size is preserved in nano regime with smallest being of 33% Sr doped $LaMnO_3$. The result of present study indicates that the molar ratio of taken precursors contained a low fraction of monodentate legend and a higher portion of C-C-O structure due to the presence of ethylene glycol, caused to obtain a small size of perovskite structure synthesized at the low sintering temperature as low as 750^0C and calcinated at 400^0C. MR study both at room temperature as well as at low temperature reveals that MR is good for x=0.33 doped $La_{1-x}Sr_xMnO_3$ perovskite. Finally, our study reveals that 33 % doped sample with average particle size 24.28 nm LSMO sample opens up a possibility of use, for room and low temperature, in low magnetic field sensor applications. Also with proper encapsulation can be used for magnetic hyperthermia.

Acknowledgements

This study was performed in National Physical Laboratory (NPL) New Delhi and Center of Excellence in Materials Sciences (Nanomaterials), Department of Applied Physics AMU, Aligarh, India.

Reference

1. S. Jin, M. McCormack, T.H. Tiefel, R. Ramesh, J. Appl. Phys. **76**, 6929 (1994) **DOI:** 10.1063/1.358119
2. B. Ll, R. Enrich, J. Mora, A. Calleja, J. Fontcuberta, X. Obradors, Appl. Phys. Lett. **69**, 1486 (1996); DOI: 10.1063/1.116916
3. J. M. T. Thompson and Michael Ziese, Phil. Trans. R. Soc. Lond. A January **15**, 137-150 (1765). **DOI:** 10.1098/rsta.2000.0524
4. A.Lussier, J. Dvorak, S. Stadler, J. Holroyd, M. Liberati, E. Arenholz, S.B. Ogale, T. Wu, T. Venkatesan, Y.U. Idzerda, Thin Solid Films **516**, 880 (2008) **DOI:** 10.1016/j.tsf.2007.04.049
5. K. Miyazaki, N. Sugimura, K. Matsuoka, Y. Iriyama, T. Abe, M. Matsuoka, Z. Ogumi, J. Power Sources **178**, 683 (2008) **DOI:** 10.1016/j.jpowsour.2007.08.007
6. L. Alvydas, S.I. Khartsev, G. Alex, Appl. Phys. Lett. **77**, 756 (2000) **DOI:** 10.1063/1.127109
7. Manh-Huong Phan, Hua-Xin peng, Seong-Cho Yu, Nguyen Duc Tho, Hoang nam Nhat, Nguyen Chau JMMM 316 (2007) 562-e565 **DOI:** 10.1016/j.jmmm.2007.03.021
8. Ravi, V., S.D. Kulkarni, V. Samuel, S.N. Kale, J. Mona,R. Rajgopal, A. Daundkar, P.S. Lahoti and R.S. Joshee, 2007. Ceramics Int., 33: 1129-1132. **DOI:** 10.1016/j.ceramint.2006.02.008
9. Kameli, P., H. Salamati and A. Aezami, 2008. J. Alloys Comp., 450: 7-11. **DOI:** 10.1016/j.jallcom.2006.10.078
10. Zhao, L. F., W. Chen, J.L. Shang, Y.Q. Wang, G.Q. Yu, X. Xiao, J.H. Miao, Z.C. Xia and S.L. Yuan, 2006. Mater. Sci. Eng. B., 127: 193-197. **DOI:** 10.1016/j.mseb.2005.10.020
11. Wang, T., X. Fang, W. Dong, R. Tao, Z. Deng, D. Li,Y. Zhao, G. Meng, S. Zhou and X. Zhu, 2008. J. Alloys Comp.,458: 248-252. **DOI:** 10.1016/j.jallcom.2007.04.023
12. Kalyana Lakshmi, Y., G. Venkataiah, M. Vithal and P. Venugopal Reddy, 2008. Phys. B., 403: 3059-3066. **DOI:** 10.1016/j.physb.2008.03.018
13. Dormann J.L., Fiorani D. and Tronc E., 1997 Adv. Chem. Phys. 98 283 **DOI:** 10.1051/jp4:19971208
14. Dormann J, Fiorani D and Tronc 1999 J Magn. Magn. Mater. **202** 251 **DOI:** 10.1016/S0304-8853(98)00627-1
15. Jonsson P e 2004 Adv. Chem. Phys. **128** 191. **DOI:** arXiv:cond-mat/0310684v2
16. Suzuki m, Fullem S I and Suzuki I S 2009 Phys. Rev. B 79 024418 **DOI:** 10.1103/PhysRevB.79.024418
17. Bedanta s and Kleemann W 2009 J. Phys. D: appl. Phys.42 013001 **DOI:** 10.1088/0022-3727/42/1/013001
18. Rudolf Hergt, Silvio Dutz, Robrt Mullr and Matthias Zeisberger J. Phys.: Condens. Mattr 18 (2006) S2919-S2934 **DOI:** 10.1088/0953-8984/18/38/S26
19. Vasseur S, duguet E, S, Hadova E, Portier J, Goglio G, Mornet S, Hadova E, Knizek K, Marysko M, Vevrka P and Pollert 2006 J. Magn. Magn, Mater. **302** 315. **DOI:** 10.1016/j.jmmm.2005.09.026
20. Uskokovic V, Kosak A and Drofenik M 2006 Mater. Lett. **60** 2620. **DOI:** 10.1016/j.matlet.2006.01.047
21. Pradhan A K , Bah R, Konda R B, Mundle R, Mustafa H, Bamiduro O, and Rakhimov R R 2008, J Appl. Phys **103** 07F704. **DOI:** 10.1063/1.2829906
22. Prasad N K, Hardel L, Duguet E and Bahadur D 2009 J Mag. Mag. Mater. **321** 1490. **DOI:** 10.1016/j.jmmm.2009.02.063
23. T. Zhang, C.G. Jin, T. Qian, X.L. Lu, J.M. Bai, X.G. Li, J. Mater. Chem. **14**, 2787 (2004)

DOI: 10.1039/B405288A
24. D. Zhu, H. Zhu, Y.H. Zhang, J. Phys.: Condens. Matter **14**, L519 (2002)
DOI: 10.1088/0953-8984/14/27/102
25. D. Zhua, H. Zhu, Y. Zhang, Appl. Phys. Lett. **80**, 1634 (2002)
DOI: 10.1063/1.1455690
26. Li K, cheng R, Wang S and Zhang Y 1998 J. phys.: Condens. Matter 10 4315
DOI: 10.1088/0953-8984/10/19/019
27. F. Gao, R. A. Lewis, X.L. Wang, S.X. Dou, J. Alloys Compd. 347, 314 (2002)
DOI: 10.1016/S0925-8388(02)00789-2
28. N.T. McDevitt, W.L. Baun, Spectrochim. Acta 20 (1964) 799
DOI: 10.1016/0371-1951(64)80079-5
29. H. Y. Hwang, S. W. Cheong, N. P. Ong, and B. Batlogg, Phys. Rev. Lett. **77**, 2041 (1996).
DOI: 10.1103/PhysRevLett.77.2041
30. P. Dey and T. K. Nath, Appl. Phys. Lett. **89**, 163102 (2006)
DOI: 10.1063/1.2362595
31. P. Dey and T. K. Nath, Appl. Phys. Lett. **87**, 162501 (2005).
DOI: 10.1063/1.2089179

